



Published in final edited form as:

Bioorg Med Chem Lett. 2017 July 15; 27(14): 3107–3110. doi:10.1016/j.bmcl.2017.05.038.

## Design, synthesis and evaluation of antitumor acylated monoaminopyrroloquinazolines

Bo Chao<sup>a,#</sup>, Bingbing X. Li<sup>a,#</sup>, and Xiangshu Xiao<sup>\*,a,b</sup>

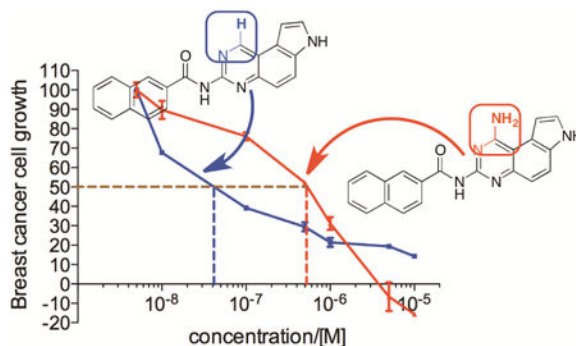
<sup>a</sup>Program in Chemical Biology, Department of Physiology and Pharmacology, Oregon Health & Science University, 3181 SW Sam Jackson Park Rd, Portland, Oregon 97239, USA

<sup>b</sup>Knight Cancer Institute, Oregon Health & Science University, 3181 SW Sam Jackson Park Rd, Portland, Oregon 97239, USA

### Abstract

Pyrroloquinazoline is a privileged chemical scaffold with diverse biological activities. We recently described a series of *N*-3 acylated 1,3-diaminopyrroloquinazolines with potent anticancer activities. The *N*-1 primary amino group in 1,3-diaminopyrroloquinazoline is critical for its inhibitory activity against dihydrofolate reductase (DHFR). In order to design out this unnecessary DHFR inhibition activity and further expand the chemical space associated with pyrroloquinazoline, we removed this *N*-1 primary amino group. In this report, we describe our design and synthesis of a series of *N*-3 acylated monoaminopyrroloquinazolines. Biological evaluation of these compounds identified a naphthamide **4a** as a potent anticancer agent (GI<sub>50</sub> = 88-200 nM), suggesting that removing the *N*-1 primary amino group in 1,3-diaminopyrroloquinazoline is a useful chemical modification that can be introduced to improve the anticancer activity.

### Graphical abstract



\*To whom correspondence should be addressed. xiaoxi@ohsu.edu; Tel:1-503-494-4748.

#These authors made equal contributions.

**Publisher's Disclaimer:** This is a PDF file of an unedited manuscript that has been accepted for publication. As a service to our customers we are providing this early version of the manuscript. The manuscript will undergo copyediting, typesetting, and review of the resulting proof before it is published in its final citable form. Please note that during the production process errors may be discovered which could affect the content, and all legal disclaimers that apply to the journal pertain.

## Keywords

anticancer; privileged scaffold; pyrroloquinazoline; reduction

Privileged chemical scaffolds possess specific biological activities against multiple disparate targets depending on the unique combination of substitution pattern on the scaffold.<sup>1</sup> These structures are great starting points to discover small molecule ligands to different classes of biomolecules including proteins and nucleic acids.<sup>1,2</sup> Perhaps the most prominent member among the privileged scaffolds is benzodiazepine which has been shown to present numerous biological activities including  $\gamma$ -aminobutyric acid (GABA) receptor modulation,<sup>3,4</sup> cholecystinin (CCK) receptor modulation<sup>5-7</sup> and apoptosis-inducing activity.<sup>8,9</sup> In medicinal chemistry, structure-activity relationship (SAR) studies on privileged structures are generally highly productive with clearly discernible SAR patterns.<sup>1,10</sup>

We recently became interested in privileged pyrroloquinazoline scaffold to develop potential anticancer agents.<sup>2,10</sup> *7H*-Pyrrolo[3,2-*f*]quinazoline-1,3-diamine (**1**, Figure 1) was originally synthesized as a dihydrofolate reductase (DHFR) inhibitor in the 1970s.<sup>11</sup> Over the ensuing four decades, derivatives of **1** have been shown to display additional biological activities by inhibiting diverse targets including G-protein coupled protease-activated receptors (PARs),<sup>12</sup> protein tyrosine phosphatase 1B (PTP1B)<sup>13</sup> and serum paraoxonase (PON).<sup>2,14</sup> During this period, the chemical space associated with **1** was heavily investigated, most of which focused on different alkyl groups of varying hydrophobicity at *N*-7.<sup>2</sup> Recently, we further expanded the chemical space associated with **1** through developing a unique suite of methods to regioselectively mono-*N*-acylate the three nucleophilic nitrogens in **1** (i.e. *N*-1, *N*-3 and *N*-7) (Figure 1).<sup>10</sup> From this focused library of mono-*N*-acylated 1,3-diaminopyrroloquinazolines, we found that compounds **2** with an acyl group at *N*-3 are generally more potent than other acylated counterparts as antiproliferative agents in breast cancer cells.<sup>10</sup> Among these, compound **3** was the most potent inhibitor of MDA-MB-231 and MDA-MB-468 cell growth with sub-micromolar or low micromolar GI<sub>50</sub>,<sup>10</sup> a concentration required to inhibit 50% of the cell growth.

In our previous published report, we showed that compound **3** did not inhibit human DHFR although the original compound **1** did so potently.<sup>10</sup> This difference was ascribed to the presence of a bulky naphthoyl group in **3**, which could not be tolerated in the active site of DHFR.<sup>10</sup> Upon examination of reported DHFR inhibitors,<sup>15</sup> virtually all of them contain the pharmacophore of 2,4-diaminopyrimidine moiety and the amino group highlighted in **1** (Figure 1) is always a primary amino group. This primary amino group can form two hydrogen bonds with DHFR through the *N-H* functionality as a hydrogen bond donor.<sup>16</sup> Along this line of analysis, replacement of this amino group with a hydrogen atom would be expected to generate compounds devoid of DHFR inhibitory activity. Consistent with this hypothesis, replacement of 4-amino group in 2,4-diamino-6,7-diphenylpteridine with a hydrogen atom resulted in complete loss of DHFR inhibition.<sup>17</sup> Furthermore, this structural change is also expected to bring significant changes to the electrostatic potential (ESP) surfaces. As models to test this hypothesis, we optimized the structures of acetamides **2b**

and **4b** (Figure 1, R = Me) at the HF/6-31g(d,p) level of theory in Jaguar in Schrödinger modeling package. Then the ESP surfaces were calculated from their respective electron densities (Figure 2).<sup>10</sup> It is obvious that both the sterics and electronics around position 1 of the pyrroloquinazoline nucleus are significantly different between **2b** and **4b** (Figure 2), suggesting that this structural change will further enhance the diversity of the chemical space belonging to pyrroloquinazoline.<sup>2</sup> In this report, we describe the synthesis and anticancer potential of a series of such compounds **4**.

Our initial strategy to prepare **4** was to couple mono-amino compound **7** with appropriate anhydrides or NHS esters (Scheme 1). Therefore, the previously reported compound **5**<sup>10</sup> was chlorinated<sup>18</sup> with POCl<sub>3</sub> to generate **6**. Chloride **6** was not stable towards extensive workup and it was thus used directly without further purification for reduction by NaBH<sub>4</sub> in the presence of PdCl<sub>2</sub>(dppf)•DCM<sup>19</sup> to provide monoamine **7** in 16% yield. Direct coupling of **7** with NHS ester **8** at an elevated temperature (120 °C) yielded **4a** in 11% yield. Attempts to improve this coupling yield at lower or higher temperatures were unfruitful. While this route could provide desired compound **4**, the low yields in both the reduction and coupling steps prompted us to investigate an alternative route to prepare **4**.

A revised synthetic route to **4** is presented in Scheme 2. Intermediate **5** was first coupled to an NHS ester (for **9a**) or a homoanhydride (for **9b-9f**) as described before to give amides **9**.<sup>10</sup> The hydroxyl group in **9** was then converted into a hydrogen atom by a sequence of chlorination with POCl<sub>3</sub> followed by reduction using NaBH<sub>4</sub> catalyzed by PdCl<sub>2</sub>(dppf)•DCM to provide desired compounds **4** in reasonable yields (20-37%).<sup>20</sup> While chlorination of the aliphatic amides **9b-9f** was carried out successfully at slightly elevated temperatures (70-90 °C), we found that it was necessary to perform chlorination of aromatic amide **9a** at lower temperature (room temperature) to obtain **4a**.

With the newly synthesized compounds **4a-4f** in hand, we evaluated their potential activity in inhibiting breast cancer cell growth and compared them with the corresponding amines **2** (Table 1 and Figure 1). Two different breast cancer cell lines MDA-MB-231 and MDA-MB-468 were used for this purpose. These two cell lines represent triple-negative breast cancer (TNBC) cells and this subtype of breast cancer has the worst prognosis among the different breast cancer subtypes.<sup>21</sup> The cells were incubated with different concentrations of the compounds for 72 h. Then the number of remaining viable cells was quantified by the MTT (3-(4,5-dimethylthiazol-2-yl)-2,5-diphenyltetrazolium bromide) reagent as reported previously.<sup>22-24</sup> The drug concentrations required for 50% growth inhibition (GI<sub>50</sub>) were calculated from the corresponding dose-response curves and are presented in Table 1. The results shown in Table 1 demonstrated that the aliphatic amides **4b-4f** are in general not potent inhibitors of either cell lines with the exception of **4d**, which presented single-digit μM activities in both of the cell lines (GI<sub>50</sub> = 3.46 ± 1.46 and 2.02 ± 1.10 μM in MDA-MB-231 and MDA-MB-468, respectively) and was ~10-fold more potent than **2d**. The overall weak activity for the aliphatic amides is consistent with the weak activity observed in **2b-2e** (Table 1).<sup>10</sup> As reported previously,<sup>10</sup> compound **2a**, being a naphthamide, was the most potent congener in this focused library of compounds. Strikingly, we found that compound **4a** was even more potent than **2a** in both of the cell lines (Table 1 and Figure 3).

The  $GI_{50}$  for **4a** was  $200 \pm 170$  nM in MDA-MB-231 cells and  $80 \pm 26$  nM in MDA-MB-468 cells, which represent 5-8-fold improvement over **2a** (Figure 3), suggesting that aromatic amides of monoaminopyrroloquinazoline may be more favorable than aromatic amides of 1,3-diaminopyrroloquinazoline in delivering potent antitumor agents. In this series of amides of monoaminopyrroloquinazoline, cLogP or cell-permeability alone is insufficient to determine the antiproliferative activities. For example, while the most potent compound **4a** has the highest cLogP value (3.50) (Scheme 2), compound **4f** (cLogP = 2.08) was much less potent than **4c** (cLogP = 1.37) or **4d** (cLogP = 1.90).

In conclusion, a series of acylated monoaminopyrroloquinazolines was designed to remove a pharmacophore typically present in DHFR inhibitors. These compounds were synthesized in a facile and generally applicable strategy of coupling and reduction. The facile synthesis of these compounds allowed us to have access to further expanded chemical space associated with pyrroloquinazoline.<sup>10</sup> Evaluation of the antiproliferative activities of these compounds in two breast cancer cell lines revealed that aliphatic amides possess relative weak antiproliferative potential. On the other hand, the naphthamide **4a** represents a potent inhibitor of breast cancer cell growth. These results suggest that aromatic amides of monoaminopyrroloquinazoline can be a new class of potential cancer therapeutics.

## Acknowledgments

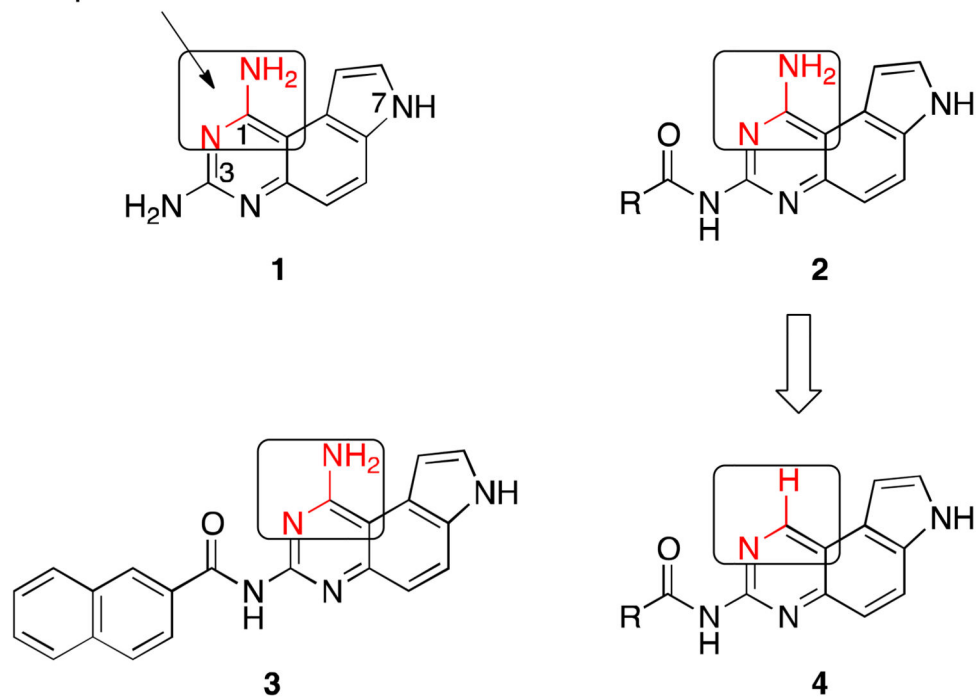
This work was made possible by the generous financial supports provided by Oregon Health & Science University (OHSU) School of Medicine, OHSU Technology Transfer and Business Development, Oregon Clinical and Translational Research Institute, Oregon Medical Research Foundation, Lloyd Fund and National Institutes of Health (R01GM122820).

## References and notes

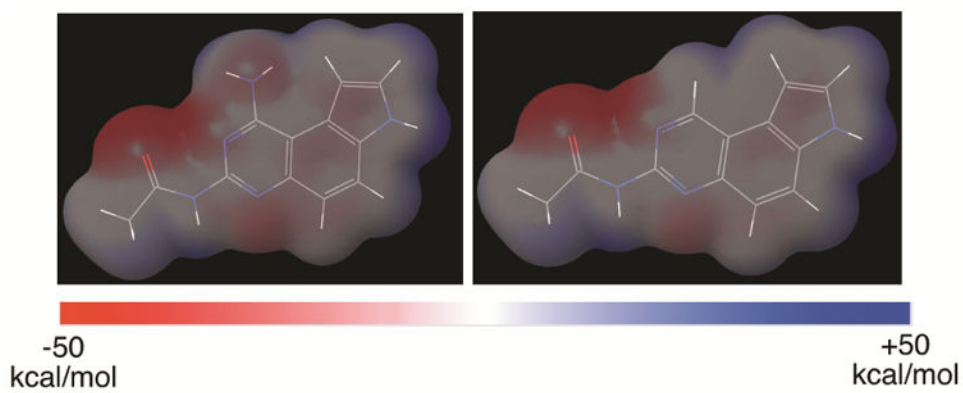
1. Welsch ME, Snyder SA, Stockwell BR. *Curr Opin Chem Biol.* 2010; 14:347–361. [PubMed: 20303320]
2. Chao B, Li BX, Xiao X. *MedChemComm.* 2015; 6:510–520. [PubMed: 25937878]
3. Sternbach LH. *J Med Chem.* 1979; 22:1–7. [PubMed: 34039]
4. Sigel E. *Curr Top Med Chem.* 2002; 2:833–839. [PubMed: 12171574]
5. Evans BE, Rittle KE, Bock MG, DiPardo RM, Freidinger RM, Whitter WL, Lundell GF, Veber DF, Anderson PS, Chang RSL, Lotti VJ, Cerino DJ, Chen TB, Kling PJ, Kunkel KA, Springer JP, Hirshfield J. *J Med Chem.* 1988; 31:2235–2246. [PubMed: 2848124]
6. Desai AJ, Lam PC, Orry A, Abagyan R, Christopoulos A, Sexton PM, Miller LJ. *J Med Chem.* 2015; 58:9562–9577. [PubMed: 26654202]
7. Chang RS, Lotti VJ. *Proc Natl Acad Sci U S A.* 1986; 83:4923–4926. [PubMed: 3014520]
8. Blatt NB, Bednarski JJ, Warner RE, Leonetti F, Johnson KM, Boitano A, Yung R, Richardson BC, Johnson KJ, Ellman JA, Opiari AW Jr, Glick GD. *J Clin Invest.* 2002; 110:1123–1132. [PubMed: 12393848]
9. Boitano A, Ellman JA, Glick GD, Opiari AW Jr. *Cancer Res.* 2003; 63:6870–6876. [PubMed: 14583485]
10. Chen J, Kassenbrock A, Li BX, Xiao X. *Medchemcomm.* 2013; 4:1275–1282. [PubMed: 24163729]
11. Ledig, KW. *U S., Ed U.S.*. 1978.
12. Ahn HS, Arik L, Boykow G, Burnett DA, Caplen MA, Czarniecki M, Domalski MS, Foster C, Manna M, Stamford AW, Wu Y. *Bioorg Med Chem Lett.* 1999; 9:2073–2078. [PubMed: 10450984]

13. Cheung AW, Banner B, Bose J, Kim K, Li S, Marcopulos N, Orzechowski L, Sergi JA, Thakkar KC, Wang BB, Yun W, Zwingelstein C, Berthel S, Olivier AR. *Bioorg Med Chem Lett*. 2012; 22:7518–7522. [PubMed: 23122867]
14. Aviram M, Rosenblat M, Bisgaier CL, Newton RS, Primo-Parmo SL, La Du BN. *J Clin Invest*. 1998; 101:1581–1590. [PubMed: 9541487]
15. Debnath AK. *J Med Chem*. 2002; 45:41–53. [PubMed: 11754578]
16. Tosso RD, Andujar SA, Gutierrez L, Angelina E, Rodriguez R, Noguerras M, Baldoni H, Suvire FD, Cobo J, Enriz RD. *Journal of chemical information and modeling*. 2013; 53:2018–2032. [PubMed: 23834278]
17. McCormack JJ, Jaffe JJ. *J Med Chem*. 1969; 12:662–668. [PubMed: 5793158]
18. Sirisoma N, Pervin A, Zhang H, Jiang S, Willardsen JA, Anderson MB, Mather G, Pleiman CM, Kasibhatla S, Tseng B, Drewe J, Cai SX. *J Med Chem*. 2009; 52:2341–2351. [PubMed: 19296653]
19. Chelucci G, Figus S. *Journal of Molecular Catalysis A: Chemical*. 2014; 393:191–209.
20. The characterization data are below. **4a**: m.p. >250 °C. <sup>1</sup>H NMR (400 MHz, DMSO-*d*<sub>6</sub>) δ 11.91 (s, 1 H), 11.19 (s, 1 H), 9.89 (s, 1 H), 8.70 (s, 1 H), 7.99–8.13 (m, 5 H), 7.59–7.70 (m, 3 H), 7.54 (d, *J* = 8.9 Hz, 1 H), 7.26–7.32 (m, 1 H); <sup>13</sup>C NMR (100 MHz, DMSO-*d*<sub>6</sub>) δ 165.64, 156.85, 153.20, 148.01, 134.49, 132.12, 132.05, 131.79, 129.17, 128.79, 127.97, 127.94, 127.66, 126.79, 126.39, 124.74, 122.24, 121.22, 119.54, 116.66, 101.04. **4b**: m.p. >250 °C. <sup>1</sup>H NMR (400 MHz, DMSO-*d*<sub>6</sub>) δ 11.86 (s, 1 H), 10.52 (s, 1 H), 9.77 (s, 1 H), 8.03 (d, *J* = 8.9 Hz, 1 H), 7.60 (t, *J* = 2.7 Hz, 1 H), 7.45 (d, *J* = 8.9 Hz, 1 H), 7.19–7.26 (m, 1 H), 2.25 (s, 3 H); <sup>13</sup>C NMR (100 MHz, DMSO-*d*<sub>6</sub>) δ 169.06, 156.88, 152.94, 147.83, 131.81, 126.30, 122.19, 121.26, 119.41, 116.16, 100.85, 24.55. **4c**: m.p. 229–230 °C. <sup>1</sup>H NMR (400 MHz, DMSO-*d*<sub>6</sub>) δ 11.87 (s, 1 H), 10.48 (s, 1 H), 9.77 (s, 1 H), 8.03 (d, *J* = 8.9 Hz, 1 H), 7.59 (t, *J* = 2.5 Hz, 1 H), 7.44 (d, *J* = 8.9 Hz, 1 H), 7.22 (s, 1 H), 2.55 (q, *J* = 7.5 Hz, 2 H), 1.09 (t, *J* = 7.5 Hz, 3 H); <sup>13</sup>C NMR (100 MHz, DMSO-*d*<sub>6</sub>) δ 172.38, 156.83, 152.94, 147.86, 131.78, 126.26, 122.14, 121.24, 119.39, 116.13, 100.82, 29.57, 9.41. **4d**: m.p. 217–218 °C. <sup>1</sup>H NMR (400 MHz, DMSO-*d*<sub>6</sub>) δ 11.85 (s, 1 H), 10.49 (s, 1 H), 9.77 (s, 1 H), 8.02 (d, *J* = 9.0 Hz, 1 H), 7.60 (t, *J* = 2.7 Hz, 1 H), 7.44 (d, *J* = 8.9 Hz, 1 H), 7.23 (s, 1 H), 2.49–2.53 (m, 2 H), 1.57–1.69 (m, 2 H), 0.94 (t, *J* = 7.4 Hz, 3 H); <sup>13</sup>C NMR (100 MHz, DMSO-*d*<sub>6</sub>) δ 171.44, 156.82, 152.91, 147.86, 131.79, 126.27, 122.13, 121.25, 119.41, 116.17, 100.84, 38.22, 18.31, 13.76. **4e**: m.p. 221–222 °C. <sup>1</sup>H NMR (400 MHz, DMSO-*d*<sub>6</sub>) δ 11.85 (s, 1 H), 10.50 (s, 1 H), 9.77 (s, 1 H), 8.03 (d, *J* = 9.0 Hz, 1 H), 7.60 (t, *J* = 2.7 Hz, 1 H), 7.45 (d, *J* = 8.9 Hz, 1 H), 7.23 (s, 1 H), 2.82–2.98 (m, 1 H), 1.12 (d, *J* = 6.8 Hz, 6 H); <sup>13</sup>C NMR (100 MHz, DMSO-*d*<sub>6</sub>) δ 175.13, 156.78, 152.96, 147.90, 131.81, 126.25, 122.11, 121.24, 119.42, 116.24, 100.86, 34.38, 19.42. **4f**: m.p. 191–192 °C. <sup>1</sup>H NMR (400 MHz, DMSO-*d*<sub>6</sub>) δ 11.87 (s, 1 H), 10.04 (s, 1 H), 9.80 (s, 1 H), 8.04 (d, *J* = 8.9 Hz, 1 H), 7.61 (t, *J* = 2.7 Hz, 1 H), 7.49 (d, *J* = 8.9 Hz, 1 H), 7.25 (s, 1 H), 1.26 (s, 9 H); <sup>13</sup>C NMR (100 MHz, DMSO-*d*<sub>6</sub>) δ 176.05, 156.61, 153.14, 147.96, 131.95, 126.28, 122.08, 121.14, 119.49, 116.48, 100.97, 27.05.
21. Kang SP, Martel M, Harris LN. *Curr Opin Obstet Gynecol*. 2008; 20:40–46. [PubMed: 18197004]
22. Xie F, Li BX, Kassenbrock A, Xue C, Wang X, Qian DZ, Sears RC, Xiao X. *J Med Chem*. 2015; 58:5075–5087. [PubMed: 26023867]
23. Li BX, Yamanaka K, Xiao X. *Bioorg Med Chem*. 2012; 20:6811–6820. [PubMed: 23102993]
24. Li BX, Xie F, Fan Q, Barnhart KM, Moore CE, Rheingold AL, Xiao X. *ACS Med Chem Lett*. 2014; 5:1104–1109. [PubMed: 25313320]

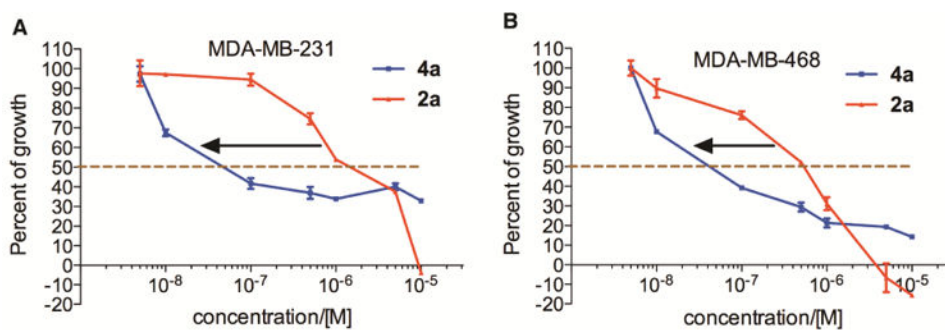
required for DHFR inhibition



**Figure 1.**  
Chemical structures of 1,3-diaminopyrroloquinazolines **1-3** and acylated monoaminopyrroloquinazolines **4**.

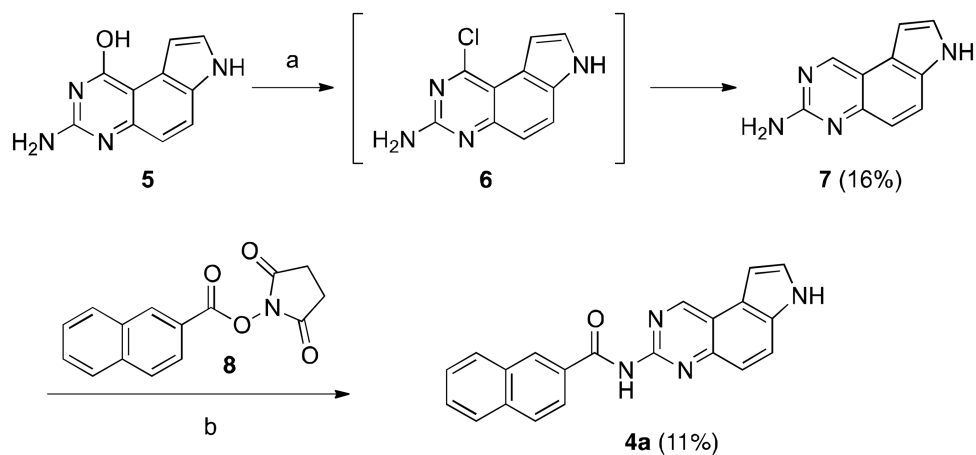


**Figure 2.** The electrostatic potential (ESP) surface maps of compounds **2b** and **4b**. The structures were optimized at HF/6-31g(d,p) level of theory implemented in Jaguar (Schrödinger) and the ESP was calculated from mapping the electron density data computed at the HF/6-31g(d,p) level of theory. The surfaces were normalized from  $-50$  kcal/mol to  $+50$  kcal/mol.

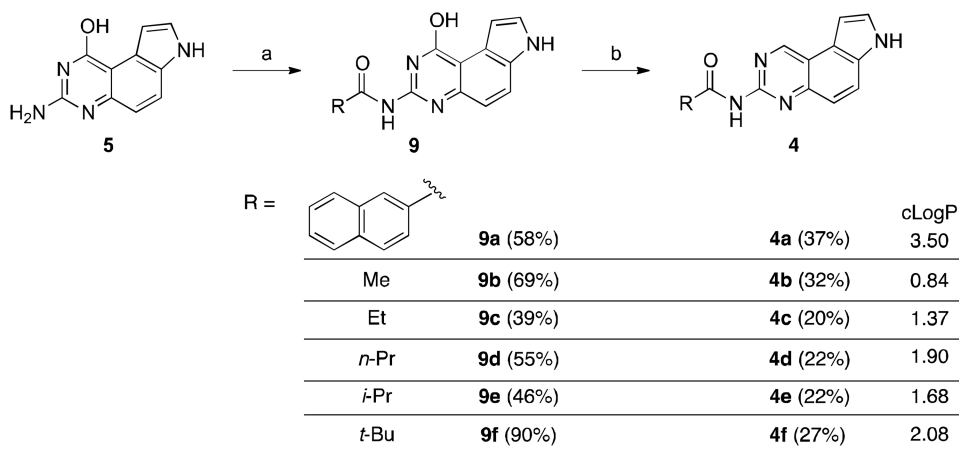


**Figure 3.** Dose-dependent antiproliferative activity of **2a** and **4a** in MDA-MB-231 (A) and MDA-MB-468 cells (B). The cells were incubated with increasing concentrations of compounds **2a** and **4a** for 72 h. Then the number of viable cells was quantified spectrophotometrically by the MTT reagent.



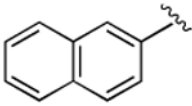
**Scheme 1.**

Initial synthesis of **4a**. Reagents and conditions: a. 1)  $\text{POCl}_3$ ,  $90^\circ\text{C}$ , overnight; 2)  $\text{PdCl}_2(\text{dppf})\cdot\text{DCM}$ ,  $\text{NaBH}_4$ ,  $\text{TMEDA}$ ,  $\text{THF}$ , r.t., 16 h; b.  $\text{DIPEA}$ ,  $\text{DMF}$ ,  $120^\circ\text{C}$ .

**Scheme 2.**

Synthesis of compounds **4** by coupling and reduction. Reagents and conditions: a. anhydrides or NHS ester **8**, DMF, 110 °C, 3 h; b. 1) POCl<sub>3</sub>, DIPEA, 1,4-dioxane, 70-90 °C, overnight (for **4b-4f**) or r.t., 4 h (for **4a**); 2) PdCl<sub>2</sub>(dppf)•DCM, NaBH<sub>4</sub>, TMEDA, THF, r.t., 16-48 h. cLogP values for **4a-4f** were calculated from ChemBioDraw Ultra 12.0.

**Table 1**Antiproliferative activities (GI<sub>50</sub>, μM) of compounds **2** and **4** in breast cancer cells.<sup>a</sup>

-R	MDA-MB-231		MDA-MB-468	
	Series 2 <sup>b</sup>	Series 4	Series 2 <sup>b</sup>	Series 4
 <b>(a)</b>	<b>1.60 ± 0.51</b>	<b>0.20 ± 0.17</b>	<b>0.44 ± 0.14</b>	<b>0.088 ± 0.026</b>
Me <b>(b)</b>	27.17 ± 11.40	>100 <sup>c</sup>	53.54 ± 29.54	>100 <sup>c</sup>
Et <b>(c)</b>	21.43 ± 9.86	72.84 ± 5.64	24.41 ± 3.33	28.30 ± 7.05
<i>n</i> -Pr <b>(d)</b>	25.52 ± 9.93	3.46 ± 1.46	27.37 ± 4.52	2.02 ± 1.10
<i>i</i> -Pr <b>(e)</b>	39.66 ± 22.46	>100 <sup>c</sup>	29.80 ± 8.41	>100 <sup>c</sup>
<i>t</i> -Bu <b>(f)</b>	N/A <sup>d</sup>	>100 <sup>c</sup>	N/A <sup>d</sup>	>100 <sup>c</sup>

<sup>a</sup>The antiproliferative activities of the compounds were assessed using the MTT assay. The cells were incubated with different concentrations of the drugs for 72 h. Then the number of viable cells was quantified by the MTT reagent. The GI<sub>50</sub>s, presented as mean ± SD (standard deviation), were calculated from the corresponding dose-response curves in Prism 5.0 using non-linear regression analysis. The SD was calculated from at least two independent measurements.

<sup>b</sup>The GI<sub>50</sub>s for series **2** were from ref<sup>10</sup>.

<sup>c</sup>The GI<sub>50</sub> was not reached at the highest tested concentration (100 μM).

<sup>d</sup>This compound was not assessed.